

## A Distinctive Fatigue Failure Criterion

Ghazi Al-Khateeb<sup>1</sup> and Aroon Shenoy<sup>2</sup>

### Abstract

This paper presents a new fatigue failure criterion for asphalt paving mixtures that is simple, unique, and distinctive. Bending beam fatigue testing in the controlled strain mode at a 1000-microstrain level and 19C temperature was performed on eleven asphalt mixtures that included unmodified and modified binders. Analysis of fatigue load-deformation raw data for each fatigue load cycle was conducted to determine the true point of fatigue failure.

With application of a sinusoidal strain on a sample, a sinusoidal response stress is expected even for a heterogeneous material like asphalt concrete. In such a case, a smooth traditional load-deformation (or stress-strain) hysteresis loop is anticipated. This holds true as long as there is no fatigue damage induced in the material. With repeated load applications, the sample starts to fatigue and microcracks are induced. These microcracks introduce discontinuities in the stress paths and the stress response starts to distort. This gets reflected in the load-deformation hysteresis loop, which in turn shows this distortion. Similar distortion can also be seen by observing the sinusoidal load-deformation waveform, where the stress response is no longer dependent on the strain input due to the formation of interconnected fatigue cracks. By tracking the distortion in the hysteresis loop or in the waveform, one is able to get a clear indication of when the first microcracks appeared, and how they progressed up to the point of complete fatigue failure.

**Key Words:** Fatigue Failure, Failure Criterion, Fatigue Damage, Repeated Loading, Hysteresis Loop, Waveform.

---

<sup>1</sup> Senior Research Engineer, SaLUT Inc., Turner-Fairbank Highway Research Center (TFHRC), McLean, VA 22101, [Ghazi.Al-Khateeb@fhwa.dot.gov](mailto:Ghazi.Al-Khateeb@fhwa.dot.gov).

<sup>2</sup> Senior Research Rheologist, SaLUT Inc., TFHRC, McLean, VA 22101, [Aroon.Shenoy@fhwa.dot.gov](mailto:Aroon.Shenoy@fhwa.dot.gov).

## Introduction

Fatigue failure is known to occur when asphalt pavements undergo repeated loading in the intermediate temperature range from roughly 10C to 30C. Considerable research has been done to develop theoretical models, experimental laboratory testing techniques, and data analysis methods to predict the fatigue performance of asphalt paving mixtures (1-58).

The focus of the present paper is to seek a true definition and a distinctive criterion of fatigue failure for asphalt paving mixtures. The data analysis method and hence the discussion are limited to the various approaches that have been proposed in the literature for analyzing laboratory fatigue data and identifying the point of fatigue failure.

The fatigue behavior of asphalt mixtures is generally established using a bending beam fatigue test. Failure (or the number of cycles to failure) in fatigue testing has been defined in various ways and sometimes arbitrarily, and the value cited depends on the mode of loading. For this reason, some researchers, e.g., Monismith and Deacon (1) corrected for the mode of loading by introducing a mode factor in the analysis of fatigue testing. Many researchers considered the initial stiffness reduction in fatigue testing as a measure of fatigue failure. Others observed crack propagation to track fatigue failure. And some others introduced dissipated energy concepts to define fatigue failure.

In the constant stress mode of testing, some researchers, e.g., Pell and Cooper (2) and Tayebali et al. (3), defined fatigue failure as the complete fracture at the end of the fatigue test when the specimen fails due to tensile strains. Other researchers such as Rowe (4) defined fatigue failure as occurring when the initial complex modulus has been reduced by 90 percent. Van Dijk (5) defined fatigue failure as occurring when the initial strain doubled.

In the constant strain mode, since the strain stays constant and the stress decreases during the fatigue test, defining fatigue failure is harder. Again researchers have adopted several different fatigue failure definitions. The most common and widely used definition for fatigue failure in the constant strain mode is the 50-percent reduction in the initial stiffness as defined by Pronk and Hopman (6) and Tayebali et al. (3, 7). A 50-percent reduction in the initial

modulus was also defined as fatigue failure by Van Dijk and Vesser (8). McCarthy (9) compared reductions in stiffness with observed crack propagation. Subsequently, the 50-percent reduction in stiffness was adopted to define the fatigue failure point by the AASHTO as a provisional standard TP8-94 (10).

The SHRP test method detailed in Tayebali et al. (11) recommends plotting the logarithm of stiffness versus the logarithm of the number of load repetitions and fitting an exponential relationship of the following form:

$$\text{Stiffness} = Ae^{bN} \quad (1)$$

where:

$A$  and  $b$  = Constants;

$e$  = Base natural logarithm; and

$N$  = Number of load cycles.

Rowe and Bouldin (12) caution against the use of logarithmic plots as they can produce misleading interpretation of the data.

Besides the fatigue failure definition of 50-percent stiffness reduction, some researchers have proposed energy-based failure concepts. In the SHRP-A-404 Report (13), dissipated energy was used for fatigue analysis. The dissipated energy per cycle is computed as the area within the stress-strain hysteresis loop. This energy decreases with an increasing number of load cycles in the strain-controlled fatigue test as the stress decreases; on the other hand, the dissipated energy per cycle increases as the number of load cycles increases for the stress-controlled fatigue test.

Hopman et al. (14) proposed the use of an “Energy Ratio” concept to define fatigue failure in the controlled strain fatigue tests. They plotted the energy ratio against the number of load cycles. A significant change in the slope of the curve occurred at a critical number of load cycles, which was considered the failure point on the curve. The critical number of load cycles corresponded to a 40-percent reduction in the complex modulus. Hopman et al. (14) found evidence of crack initiation at the point where the significant change in slope occurred, i.e., deviated from a straight line.

Kim et al. (15) introduced the 50-percent reduction in pseudo stiffness as a failure point in fatigue testing, which was believed to be independent of mode of loading and stress/strain amplitude.

Rowe (4) and Rowe and Bouldin (12) used the concept of “Energy Ratio”, which was proposed by Hopman et al. (14), to define fatigue failure. The fatigue failure for the controlled stress and the controlled strain modes was identified using an “energy ratio” that was defined as the ratio of the dissipated energy in the first cycle times the number of cycles (N) to the dissipated energy in the N-th cycle.

Ghuzlan and Carpenter (16) proposed a “Dissipated Energy” concept to define fatigue failure in asphalt mixtures. They used the ratio of the change in dissipated energy between two consecutive cycles (N, N+1) to the total dissipated energy in the load cycle N. This new method was believed to define fatigue failure independently of the mode of loading in fatigue testing. Failure was selected as the point where this ratio increased rapidly after a consistent stable trend for this ratio with load cycles.

### **Objectives**

The main objectives of this study are:

1. To evaluate existing approaches for fatigue failure;
2. To discuss the limitations of the evaluated approaches; and
3. To present a new fatigue failure criterion, which is fundamental, simple, and distinctive.

### **Materials, Experimental Plan and Methodology**

#### ***Aggregate***

The aggregate consisted of 92-percent crushed diabase and 8-percent quartz and quartzite natural sand as shown in Table 1. The aggregate gradation is shown in Figure 1. It met the 1991 Virginia Department of Transportation (VDOT) specifications for surface mixtures (SM-3).

**Table 1 Aggregate Properties for the Diabase**

<b>Percent Passing (%)</b>			
<b>Sieve Size (mm)</b>	<b>92 % Diabase</b>	<b>8 % Natural Sand</b>	<b>Blend</b>
25.0	100.0		100.0
19.0	98.6		98.7
12.5	73.9		76.0
9.5	58.7	100.0	62.0
4.75	39.5	95.8	44.0
2.36	27.2	88.2	32.1
1.18	19.4	74.8	23.8
0.600	14.4	46.0	16.9
0.300	11.1	14.1	11.3
0.150	8.2	4.8	7.9
0.075	5.7	2.9	5.5
<b>Specific Gravity and Percent Absorption</b>			
Bulk Dry SG <sup>1</sup>	2.933	2.565	2.892
Bulk SSD <sup>2</sup>	2.956	2.601	2.916
Apparent SG <sup>1</sup>	3.002	2.659	2.961
% Absorption	0.8	1.4	0.8
<b>Flat and Elongated Particles at 3-to-1 Length-to-Thickness Ratio, Percent by Mass</b>			
	21	NA <sup>3</sup>	
<b>Los Angeles Abrasion, Percent Loss by Mass</b>			
	14	NA <sup>3</sup>	
<b>Fine Aggregate Angularity</b>			
	49	45	

<sup>1</sup> Specific Gravity<sup>2</sup> Saturated Surface Dry<sup>3</sup> Not Applicable

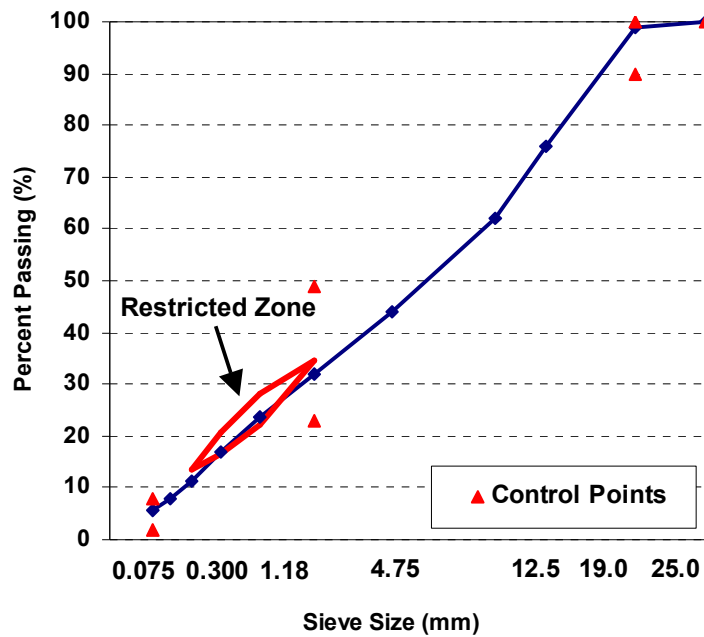


**Figure 1. Diabase Aggregate Gradation Plotted on a 0.45 Power Chart**

### ***Binders***

Eleven binders have been used in this study. They included a PG64-22 and a PG70-22 (unmodified binders), a PG70-28 (air-blown), and eight polymer-modified binders of PG70-28, which consisted of the following polymers: Terpolymer (Elvaloy), Styrene-Butadiene-Styrene Linear-Grafted, Styrene-Butadiene-Styrene Linear, Styrene-Butadiene-Styrene Radial-Grafted, Ethylene-Vinyl Acetate, Ethylene-Vinyl-Acetate Grafted, Ethylene Styrene Interpolymer, and Chemically Modified Crumb Rubber. The PG numbers shown are based on the Superpave system description. All the binders were from the same source, a Venezuelan crude (blend of Boscan and Bachaquero). The air-blown PG70-28 was obtained by noncatalytic air blowing of a PG52-28. The polymer-modified grades were obtained by addition of various amounts of different polymers to the PG64-22, the PG52-28, or a mixture of the PG64-22 and the PG52-28 in

appropriate proportions; the goal was to achieve a PG70-28 performance grade. All of the binders were part of an extensive ongoing polymer research program at the Federal Highway Administration's Turner-Fairbank Highway Research Center in McLean, Virginia.

### ***Sample Preparation***

The binders were heated to 163C and mixed with heated aggregates in proportion to achieve a binder content of 4.85 percent by the total mass of the mixture.

All asphalt mixtures were short-term oven aged for 2 hours at 135C according to the AASHTO provisional practice PP2-00 (59) and compacted, using a Slab-Pak<sup>TM</sup> linear kneading compactor, into 180- by 500- by 50-mm slabs. Two beams, each 63-mm wide, 50-mm tall and 380-mm long with smooth faces, were then cut from each slab. The target air-void level was  $7.0 \pm 0.5$  percent. The air-void level in the sawed beam specimens was determined, and those beams having air voids outside the specified range were discarded.

All asphalt mixtures were tested approximately forty-eight hours after compaction.

### ***Testing Procedure***

Bending beam fatigue tests were performed according to the AASHTO provisional test method TP8-94 (10). The tests were conducted in the strain-controlled mode at a high strain level of 1000 microstrains and at a test temperature of 19C. The beam fatigue test device is shown in Figure 2.

The beam fatigue test was conducted according to the AASHTO TP8-94 protocol. A vertical repeated sinusoidal displacement was applied at a frequency of 10 Hz with no rest periods. The fatigue test was designed to run up to approximately 300,000 load cycles. Three to five replicates were used for each asphalt mixture at the 1000-microstrain level.

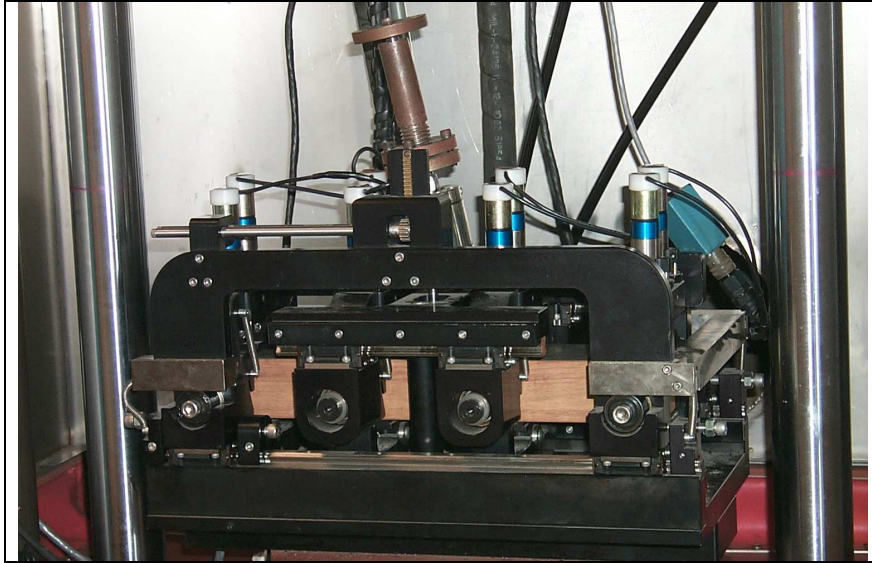


**Figure 2. Bending Beam Fatigue Test Device**

Two concentrated and symmetrical loads are applied on the fatigue beam specimen, as shown in Figures 3 and 4. The beam specimen is forced back to its original position at the end of each load pulse. It is subjected to 4-point bending. Free rotation and horizontal translation are allowed at all load and reaction points, as shown in Figure 5.

The data acquisition software (TestStar<sup>TM</sup>) of the device recorded the load and the deformation of the specimen. Tensile strains and stresses were calculated using the following equations:

$$\varepsilon_t = \frac{12d \times h}{3l^2 - 4a^2} \quad (2a)$$

where:

$\varepsilon_t$  = maximum tensile strain;

$d$  = maximum vertical deformation at the center of the beam;

$h$  = average specimen height;

$l$  = length of beam between outside clamps; and

$a$  = space between inside clamps =  $l/3$ .



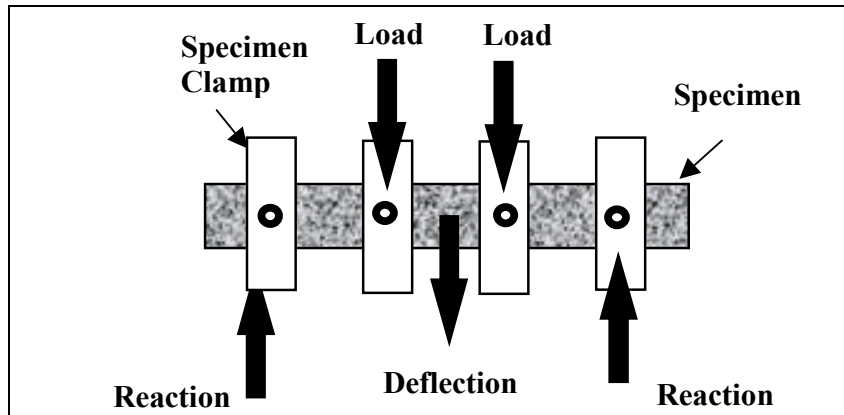


Figure 3. Bending Beam Fatigue Test Schematic Diagram

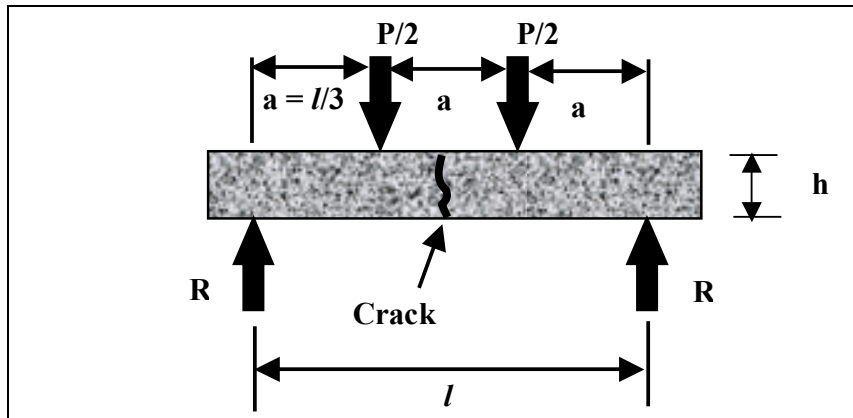


Figure 4. Loading and Geometry

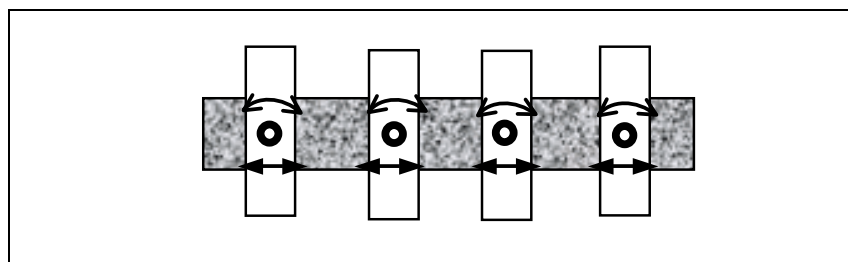


Figure 5. Freedom Conditions of Bending Beam Fatigue Test

$$\sigma_t = \frac{lP}{bh^2} \quad (2b)$$

where:

$\sigma_t$  = maximum tensile stress;

$P$  = load applied by actuator; and

$b$  = average specimen width.

Flexural stiffness ( $S$ ) was calculated using the equation given below:

$$S = \frac{\sigma_t}{\varepsilon_t} \quad (3)$$

## Results and Discussion

Applied strains, response stresses, and flexural stiffnesses were determined from the load and deformation amplitude, the geometry of the tested beam, and the distance between the beam supports.

The fatigue data obtained on the various asphalt mixtures were then analyzed using three of the existing approaches discussed previously. Table 2 summarizes the results using the three methods for all asphalt mixtures used in the study. The last column of the table shows the point of fatigue failure defined by the criterion that is proposed and discussed later in the present paper.

In the first method, the number of load cycles to fatigue failure was determined using the 50-percent stiffness reduction point. The actual number of load cycles to fatigue failure can be established graphically from interpolation of fatigue data or calculated after fitting a curve to the data. In the latter case, the natural logarithm function ( $\text{Ln}$ ) of the load cycles was used to fit the stiffness versus load cycles data (Figure 6). Table 3 shows the number of load cycles to fatigue failure for all of the mixtures by both approaches.

**Table 2 Number of Load Cycles to Fatigue Failure Using Different Methods**

Asphalt Mixture	Number of Load Cycles to Fatigue Failure Using				
	AASHTO TP 8-94 (10) Method	Rowe (4) Method		Ghuzlan and Carpenter (16) Method	Proposed Method-New Criterion
		N1	Nf		
50 % Stiffness Reduction	Reduced Energy Ratio	50 % Modulus Reduction	Dissipated Energy Ratio	Distortion of Waveform or Hysteresis Loop	
<b>PG 64-28</b>	5,323	3,400	5,323	> 300,000	10,000
<b>PG 70-22</b>	3,144	2,300	3,144	> 300,000	4,000
<b>Air-Blown</b>	7,614	5,150	7,614	> 300,000	8,400
<b>Elvaloy</b>	97,389	150,000	97,389	> 300,000	217,000
<b>SBS LG</b>	9,911	7,500	9,911	> 300,000	20,000
<b>SBS L</b>	8,774	14,000	8,774	> 300,000	30,000
<b>SBS RG</b>	12,372	9,150	12,372	> 300,000	10,000
<b>EVA</b>	5,905	6,900	5,905	> 300,000	36,700
<b>EVA G</b>	7,183	6,500	7,183	> 300,000	16,700
<b>ESI</b>	10,301	8,800	10,301	> 170,000	36,700
<b>CMCRA</b>	4,158	2,850	4,158	> 300,000	8,400

The fatigue failure at the 50-percent reduction in initial stiffness in the AASHTO provisional standard TP8-94 (10) that is widely used by asphalt professionals and technologists, was arbitrarily selected. This arbitrarily chosen point does not represent the true fatigue failure in most cases and can give misleading results. In fact, observations (4) under controlled strain conditions show the stiffness of a tested cantilever beam fell to 50 percent of its original value without any visible sign of a crack on the beam. Also the fatigue life obtained from the constant stress mode is different (lower) than the fatigue life obtained from the constant strain mode.

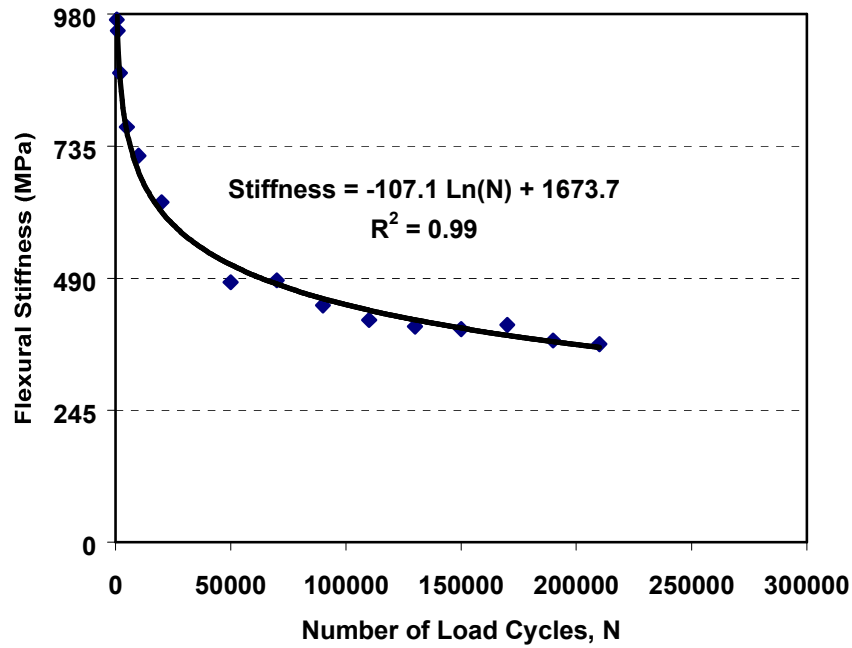


**Figure 6. Flexural Stiffness vs. Load Cycles for Elvaloy-Replicate 1**

**Table 3 Number of Load Cycles to Failure based on 50-Percent Stiffness Reduction**

Asphalt Mixture	Interpolated from Actual Data	Using Ln Function
PG 64-28	5,323	8,439
PG 70-22	3,144	4,702
Air-Blown	7,614	10,871
Elvaloy	97,389	68,160
SBS LG	9,911	11,193
SBS Linear	8,774	9,783
SBS RG	12,372	9,610
EVA	5,905	8,713
EVA Grafted	7,183	8,890
ESI	10,301	10,037
CMCRA	4,158	5,994

Rowe (4) and Rowe and Bouldin (12) used the concept of “Energy Ratio” to derive a “Reduced Energy Ratio” that was used to define fatigue failure in the controlled stress and the controlled strain modes. The “energy ratio” was defined as the ratio of the dissipated energy in the first cycle times the number of cycles (N) to the dissipated energy in the N-th cycle.

In Rowe and Bouldin analysis of fatigue failure (12), an assumption was made that the phase angle,  $\delta$ , does not change through the beam fatigue test such that the ratio of  $\sin(\delta_1) / \sin(\delta_N)$  is unity in order to derive the reduced energy ratio from the energy ratio. This assumption, however, is not always valid as the phase angle in the beam fatigue test is not constant throughout the test.

The energy ratio ( $W_N$ ) defined in Equation (4) below was used to derive the reduced energy ratio for the stress- and strain-controlled fatigue tests:

$$W_N = \frac{Nw_1}{w_N} \quad (4)$$

where:

$W_N$  = Energy ratio;

$N$  = Cycle number;

$w_1$  = Dissipated energy in first cycle; and

$w_N$  = Dissipated energy in N-th cycle.

The dissipated energy in any cycle (i) is determined as shown in Equation (5) below:

$$w_i = \pi \sigma_i \varepsilon_i \sin \delta_i \quad (5)$$

where:

$w_i$  = Dissipated energy in ith cycle;

$\sigma_i$  = Stress in ith cycle;

$\varepsilon_i$  = Strain in ith cycle; and

$\delta_i$  = Phase angle in ith cycle.

The reduced energy ratio was derived from the energy ratio in Equation (4) using Equation (5) assuming  $\sin(\delta_1) / \sin(\delta_N)$  is unity. For the stress-controlled fatigue test, Equation (6) shows the reduced energy ratio ( $R_N^\sigma$ ) as a function of the cycle number (N)

and the complex modulus in the Nth cycle ( $E_N^*$ ) as derived in Rowe and Bouldin (12):

$$R_N^\sigma = NE_N^* \quad (6)$$

where:

$N$  = Cycle number;

$E_N^*$  = Magnitude of complex modulus in N-th cycle; and

$R_N^\sigma$  = Reduced energy ratio in N-th cycle for the stress-controlled fatigue test.

Thus, in the stress-controlled fatigue test, Rowe and Bouldin (12) defined the reduced energy ratio ( $R_N^\sigma$ ) as the energy ratio ( $W_N$ ) multiplied by the modulus in the first cycle ( $E_1^*$ ).

For the strain-controlled fatigue test, the same researchers established the reduced energy ratio ( $R_N^\epsilon$ ) as a function of the cycle number ( $N$ ) and the modulus in the Nth cycle ( $E_N^*$ ), as shown in Equation (7) below:

$$R_N^\epsilon = \frac{N}{E_N^*} \quad (7)$$

where:

$R_N^\epsilon$  = Reduced energy ratio in N-th cycle for the strain-controlled fatigue test.

Thus, in the strain-controlled fatigue test, they defined the reduced energy ratio ( $R_N^\epsilon$ ) as the energy ratio ( $W_N$ ) divided by the modulus in the first cycle ( $E_1^*$ ). In other words, Rowe and Bouldin (12) used two different definitions for the reduced energy ratio in the stress- and strain-controlled fatigue tests, respectively.

In Rowe (4), the reduced energy ratio in the stress-controlled fatigue test ( $R_N^\sigma$ ) was again defined as the energy ratio ( $W_N$ ) multiplied by the initial modulus ( $E_1^*$ ), assuming that  $\sin(\delta_1) / \sin(\delta_i)$  is unity. Here, however, the reduced energy ratio in the strain-controlled fatigue test ( $R_N^\epsilon$ ) was defined as the energy ratio ( $W_N$ ) divided by the initial loss modulus ( $E_1^* \sin \delta_1$ ), assuming that the loss modulus at any cycle  $i$  ( $E_i''$ ) is approximately equal to the complex modulus at cycle  $i$  ( $E_i^*$ ); this implies that the phase angle at any cycle  $i$  is constant at 90 degrees.

Thus, two different definitions for the reduced energy ratio in the stress- and strain-controlled fatigue tests were used in both Rowe and Bouldin (12) and Rowe (4). Moreover, the definition for the reduced energy ratio in Rowe and Bouldin (12) is different from the definition in Rowe (4) for the strain-controlled fatigue test. The assumption that the phase angle does not change was used in the derivation of the reduced energy ratio in Rowe and Bouldin (12) for the stress- and strain-controlled fatigue tests. Whereas, in Rowe (4), the same assumption was only used for the stress-controlled test, and a different assumption that the loss modulus at any cycle  $i$  ( $E_i''$ ) is approximately equal to the complex modulus at cycle  $i$  ( $E_i^*$ ), implying that the phase angle at any cycle  $i$  is constant at 90 degrees was used for the strain-controlled test.

In Rowe and Bouldin (12), the fatigue failure was defined as the point when a significant change of the slope occurs at a critical number of cycles ( $N_1$ ) in the energy ratio versus the number of load cycles plot. Using the reduced energy ratio that was derived for the stress-controlled fatigue test ( $R_N^\sigma$ ) in Rowe and Bouldin (12) as shown previously,  $N_1$  was defined as the peak point of  $R_N^\sigma$  versus the number of load cycles plot. In the strain-controlled fatigue test, although the reduced energy ratio for this mode ( $R_N^\epsilon$ ) was derived as  $N / E_N^*$  in Rowe and Bouldin (12), the term  $N / E_N^*$  was plotted against the number of load cycles to determine the fatigue failure point for the strain-controlled fatigue test.

In Rowe (4),  $N_1$  was defined as the number of load cycles to “crack initiation”. The number of load cycles to “failure condition” ( $N_f$ ) was also used to define fatigue failure. In the stress-controlled fatigue test,  $N_1$  was determined from the peak of  $R_N^\sigma$  versus the number of load cycles. On the other hand, in the strain-controlled fatigue test,  $N_1$  was defined as the point at which the slope of  $R_N^\epsilon$  versus the number of load cycles deviates from a straight line. A reduction of specimen complex modulus to 50 percent of the initial value was used to define the number of cycles to failure,  $N_f$ , in the strain-controlled fatigue test, whereas a value of 10 percent was used for the stress-controlled fatigue test.

Using Rowe (4) method, the reduced energy ratio and the modulus in the constant strain mode were plotted versus the number of load cycles for Elvaloy in Figures 7 and 8, respectively.  $N_1$  was found to be 130,000 cycles in Figure 7, and  $N_f$  was determined as 147,250 cycles in Figure 8.

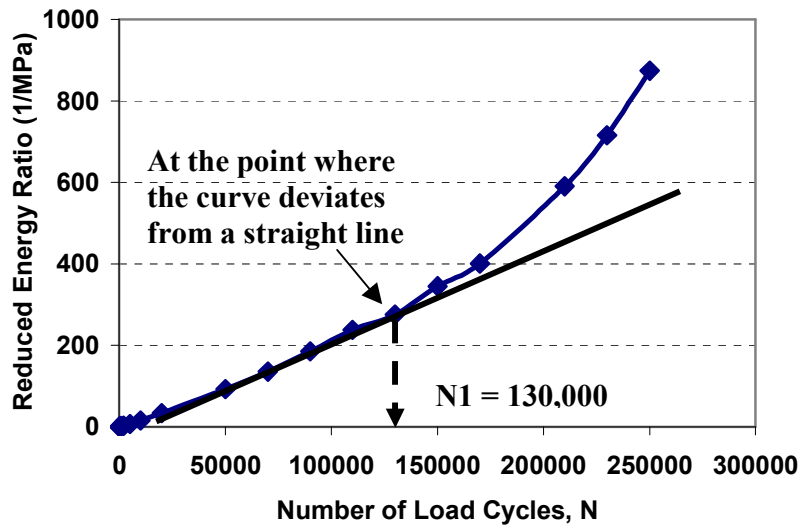


Figure 7. Reduced Energy Ratio vs. Number of Load Cycles for Elvaloy-Replicate 3

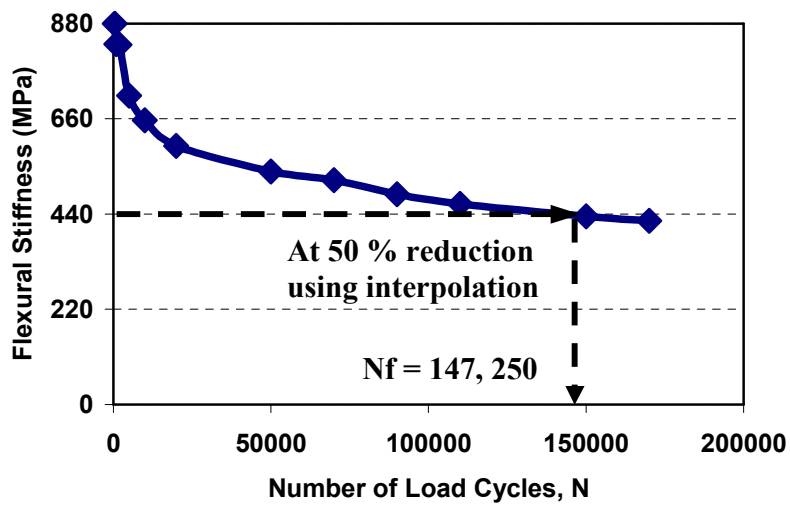


Figure 8. Flexural Stiffness vs. Number of Load Cycles for Elvaloy-Replicate 3



Similarly, Figures 9 and 10 show the reduced energy ratio and the modulus versus the number of load cycles, respectively for PG 70-22.  $N_1$  was determined from Figure 9 to be 3,800 cycles. On the other hand,  $N_f$  was determined from Figure 10 to be 5,023. It should be noted, though, that in Rowe (4)  $N_1$  was defined as the number of load cycles to “crack initiation”. On the other hand,  $N_f$  was defined as the number of load cycles to “failure condition”. This means that the event of  $N_1$  should occur before the event of  $N_f$ . This is, however, not supported by the results found using Rowe (4) method as shown in Table 2.  $N_1$  values for Elvaloy, SBS Linear, and EVA were higher than  $N_f$  values for the same mixtures, which cannot be correct. This is actually due to the fact that the assumptions used to derive the reduced energy ratio were not always valid, and the definitions of fatigue failure in Rowe (4) might not be correct.

Using the dissipated energy ratio (Ghuzlan and Carpenter [16]), the point of fatigue failure was not captured by the end of the 300,000 cycles of the fatigue test. The energy ratio decreases in the first part of the fatigue test, and then fluctuates around a flat plateau up to the end of the fatigue test. However, it should be noted that, Ghuzlan and Carpenter (16) calculated the dissipated energy ratio approximately every 100 cycles. On the other hand, in this study, the dissipated energy ratio was calculated at much longer intervals because of equipment readout limitations. This may explain why the failure could not be captured using their method. Later in this paper, fatigue failure as defined by the proposed new criterion, is shown to occur for all eleven asphalt mixtures within the 300,000 cycles of the laboratory fatigue test.

### ***Proposal of a Fundamental Fatigue Failure Criterion***

A fundamental fatigue failure criterion is proposed in this paper based on the visual observations of the load-deformation raw data. Prior researchers do not appear to have done such careful observations of raw data, and hence none have been able to propose a distinctive fatigue failure criterion as done in this work.

The fatigue data was collected under a constant strain condition, and therefore, the discussion in the following is confined to the controlled strain mode of testing.

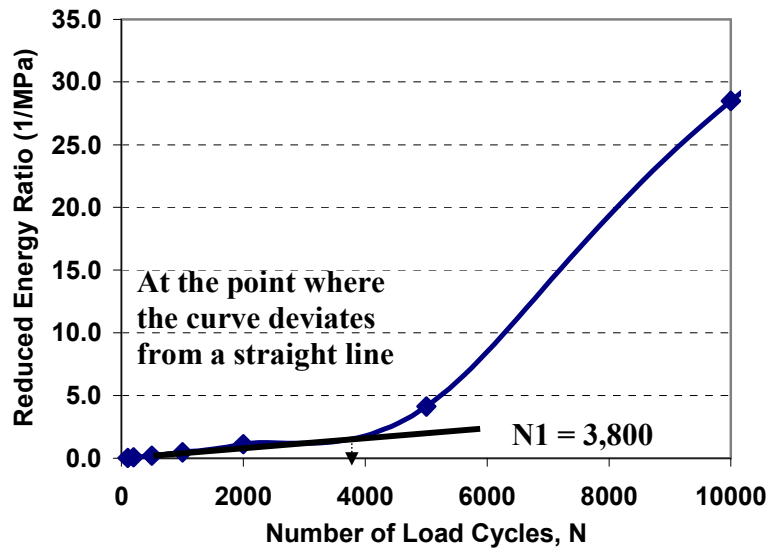


Figure 9. Reduced Energy Ratio vs. Number of Load Cycles for PG 70-22-Replicate 1

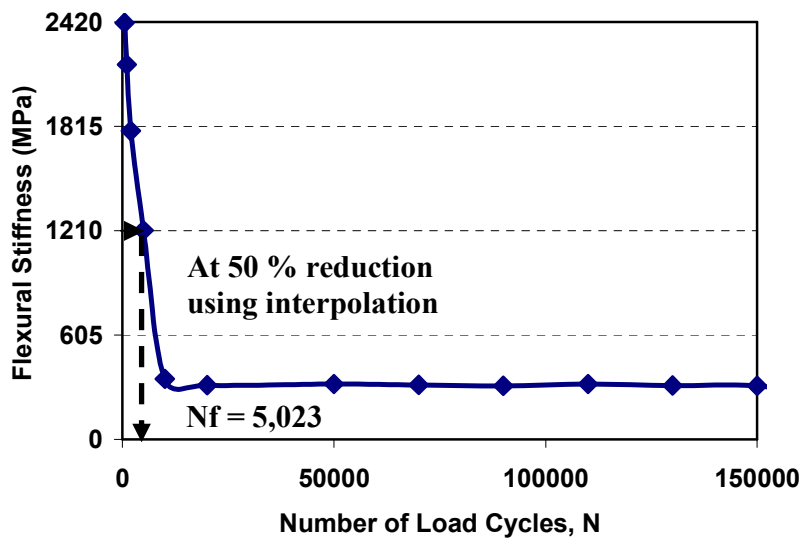
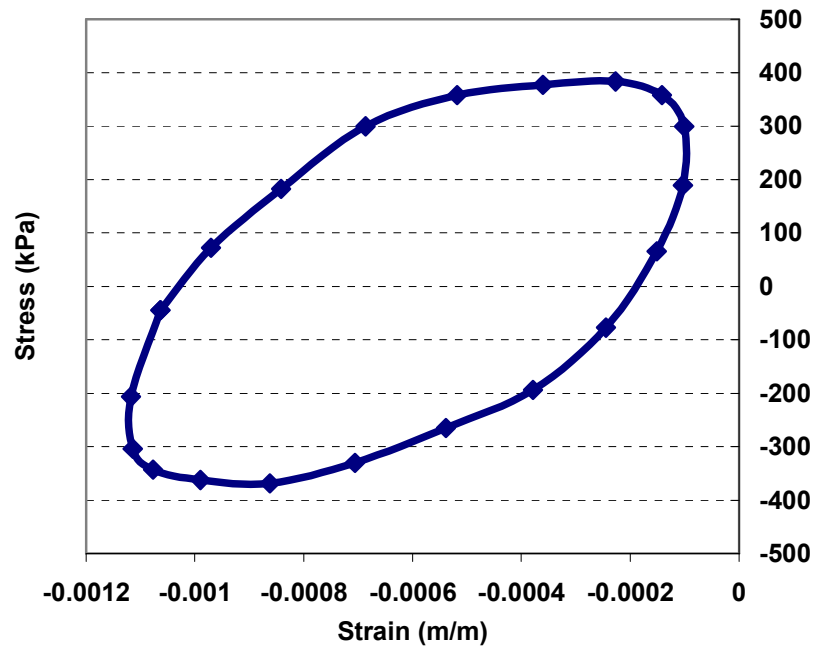


Figure 10. Flexural Stiffness vs. Number of Load Cycles for PG 70-22-Replicate 1

In a beam fatigue test, when a sinusoidal strain is applied to the sample, it is natural to expect a sinusoidal stress response even for a heterogeneous material like the asphalt concrete. This is true at the start of the test when the sample is intact and the stress paths are all well defined; at this time, the load-deformation (or stress-strain) hysteresis loop is also well defined and smooth, as shown in Figure 11. With repeated applications of strain, the material starts to fatigue and microcracks are induced in the system. These microcracks introduce discontinuities in the stress paths, and the stress response starts to distort. This can be clearly seen by observing the load-deformation (or stress-strain) hysteresis loop. Initially the distortion is slight and indicates the onset of the induced defect due to the repeated strain. When this happens the distortion of the hysteresis loop is so slight that one is likely to overlook it. However, if the hysteresis loop for each progressive cycle is observed, then it becomes obvious that this raw data is actually giving a footprint of the progression of the damage.

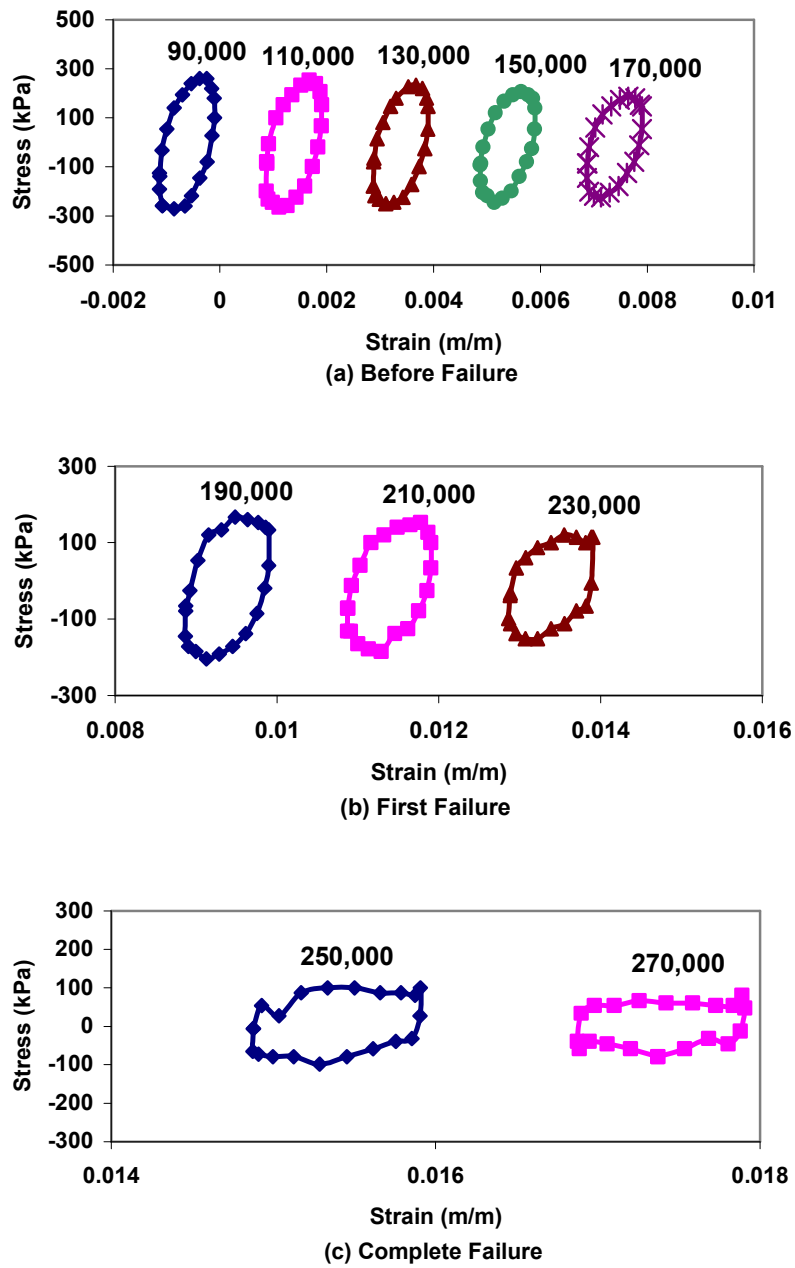


**Figure 11. Stress-Strain Hysteresis Loop**

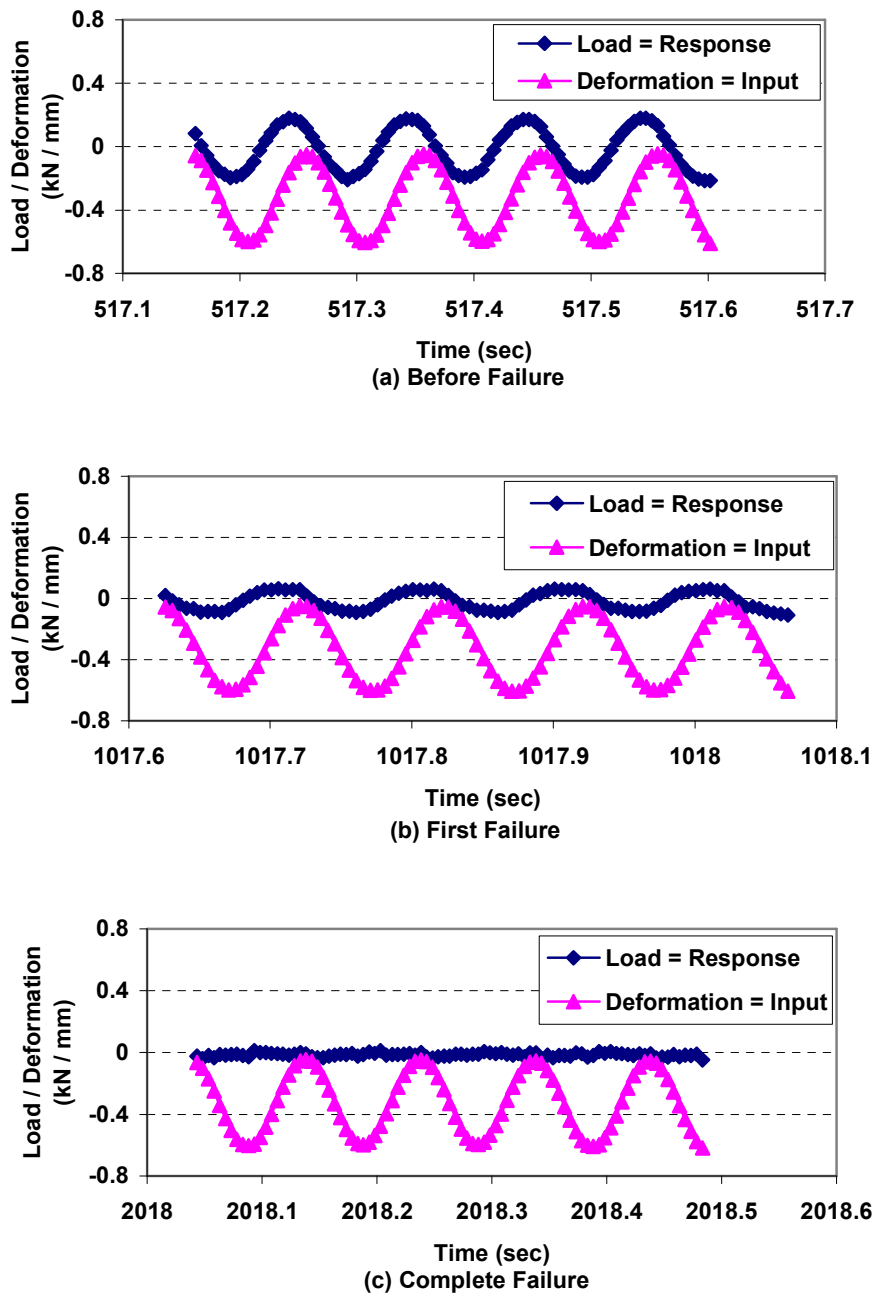
After the initial slight distortion of the stress-strain loop, the shape buckles slightly, followed by a radical change in the shape of the loop with the progress of the fatigue failure. The progression of the fatigue failure and the progressive distortions in the stress-strain hysteresis loops corresponding to selected cycle numbers are shown in Figure 12. For all mixtures tested, the appearance of the stress-strain loops were similar to those shown in Figure 12, though the distortions and the severity of distortions were different and occurred at different number of load cycles for various mixtures.

Figure 13 shows that the same information can be obtained even from the observation of the sinusoidal waveform. The input (strain or deformation) signal is smooth and well defined and stays so from the start to the end of the fatigue test. However, the response (stress or load) sinusoidal waveform starts smooth and well defined, but soon distorts and finally becomes almost flat; the latter indicates that the stress response is no longer dependent on the strain because of the discontinuities that have emerged from the cracking. The transitional point when the sinusoidal stress waveform goes from the smooth to the first level of distortion indicates the initiation of the first level of cracking (first failure). In the next few cycles, it is this initial level of cracking along with the applied strain that controls the response stress and maintains the distorted shape of the sinusoidal stress waveform. However, when the material fatigues further and the crack intensity rises, the applied strain can no longer drive the stress response and a flattened stress or load waveform is obtained, as shown in Figure 13 (complete or ultimate fatigue failure).

Using this failure criterion, the number of load cycles to failure was determined for the eleven asphalt mixtures used in this study. A comparison between results using this criterion and results using other methods are summarized in Table 2.



**Figure 12. Stress-Strain Hysteresis Loop through the Progress of Fatigue Failure for Elvaloy-Replicate 3**



**Figure 13. Load-Deformation Relationship through the Progress of Fatigue Failure for EVA Grafted-Replicate 3**

### Findings and Conclusions

This paper shows that there is no need to go through any level of calculations based on formulae for the dissipated energy or energy ratio, or rely on a somewhat arbitrary 50-percent reduction in stiffness in order to find the fatigue failure point. The fatigue failure is revealed directly from raw data by observing the distortion of the load-deformation hysteresis loop or the response waveform at the onset of the first crack appearance. Before fatigue failure, the stress and strain signals are strongly correlated and after failure, they are no longer correlated. This marks a very significant and clear definition of the point of fatigue failure. The first fatigue failure point is identified as occurring when the shape of the stress-strain (load-deformation) hysteresis loop starts to show the first signs of distortion from the original smooth oval-or-elliptical shape. The initially distorted shape typically lasts for a long period before a very irregular shape of the distorted waveform shows up. This change marks the point of the complete fatigue failure and the ultimate fatigue failure of the beam is reached.

Although the 4-point bending beam has been used to demonstrate the proposed method of analysis, the concept is not limited to only this type of fatigue testing method. It would not be unrealistic to expect such type of abrupt changes in stress-strain hysteresis loop to appear in any other fatigue testing configuration or any other material including non-bituminous and therefore, the concept could be used as a distinctive fatigue failure criterion in other cases as well. In all cases, an algorithm for sensing the onset of failure would likely need only to compute a simple “R-squared” statistic for the relationship between the stress signals for consecutive cycles with reference to the first cycle in a strain-controlled test or for the relationship between the strain signals for consecutive cycles with reference to the first cycle in a stress-controlled test, and watch for it to drop below a threshold value.

In conclusion, this new fatigue failure criterion accurately describes the true point of fatigue failure without ambiguity. It is based on the fundamental load-deformation (stress-strain) relationship of the material. No calculations of stress, strain, stiffness, or energy are needed to determine the point of fatigue failure, since it is determined directly from the raw data of the

beam fatigue testing by observing the load-deformation data within each cycle. The onset of a non-sinusoidal response in the load-deformation hysteresis loop is a simple, direct way to sense the onset of fatigue failure. Such observation of distorted hysteresis loop or waveform has never been done in the past. Indeed, this is the first time that a criterion for determining the true fatigue failure point based on fundamental raw data has been proposed. This concept is easily understood and would provide a practical way to test a pavement material for fatigue. The accuracy with which this can be done and the simplicity of the determination make it unique and distinctive.

### Acknowledgments

The authors are grateful to Mr. Scott Parobeck for making the samples and conducting the testing, and to Dr. Ernest J. Bastian, Jr., Dr. Terry Mitchell, Dr. Walaa Mogawer, Mr. Kevin Stuart, and Dr. Jack Youtcheff for their comments.

### References

1. C. L. Monismith and J. A. Deacon, "Fatigue of Asphalt Paving Mixtures", *American Society of Civil Engineers, Journal of Transportation Engineering*, TE2, pp. 317-345, 1969.
2. P. S. Pell and K. E. Cooper, "The Effect of Testing and Mix Variables on the Fatigue Performance of Bituminous Materials", *Journal of the Association of Asphalt Paving Technologists*, Vol. 44, pp. 1-37, 1975.
3. A. A. Tayebali, G. M. Rowe, and J. B. Sousa, "Fatigue Response of Asphalt-Aggregate Mixtures", *Journal of the Association of Asphalt Paving Technologists*, Vol. 61, pp. 333-360, 1992.
4. G. M. Rowe, "Performance of Asphalt Mixtures in the Trapezoidal Fatigue Test", *Journal of the Association of Asphalt Paving Technologists*, Vol. 62, pp. 344-384, 1993.



5. W. Van Dijk, "Practical Fatigue Characterization of Bituminous Mixes", *Journal of the Association of Asphalt Paving Technologists*, Vol. 44, pp. 38-72, 1975.
6. A. C. Pronk and P. C. Hopman, "Energy Dissipation: The Leading Factor of Fatigue", *Highway Research: Sharing the Benefits. Proceedings of the Conference, the United States Strategic Highway Research Program*, London, 1990.
7. A. A. Tayebali, J. A. Deacon, J. S. Coplantz, and C. L. Monismith, "Modeling Fatigue Response of Asphalt-Aggregate Mixes", *Journal of the Association of Asphalt Paving Technologists*, Vol. 62, pp. 385-421, 1993.
8. W. Van Dijk and W. Visser, "The Energy Approach to Fatigue for Pavement Design", *Journal of the Association of Asphalt Paving Technologists*, Vol. 46, pp. 1-37, 1977.
9. P. F. McCarthy, "Factors Affecting the Fatigue Characteristics of Bitumen Sand Mixtures", *Ph. D. Thesis, University of Nottingham, UK*, 1960.
10. AASHTO TP8-94, "Method for Determining the Fatigue Life of Compacted Hot-Mix Asphalt (HMA) Subjected to Repeated Flexural Bending", *AASHTO Provisional Standards*, May 2002.
11. A. A. Tayebali, J. A. Deacon, J.S. Coplantz, J. T. Harvey, and C. L. Monismith, "Fatigue Response of Asphalt-Aggregate Mixes, Part 1 – Test Method Selection", *Report SHRP-A-003A, Strategic Highway Research Program, National Research Council, Washington D. C.*, November 1992.
12. G. M. Rowe and M. G. Bouldin, "Improved Techniques to Evaluate the Fatigue Resistance of Asphaltic Mixtures", *Proceedings of 2<sup>nd</sup> Eurasphalt & Eurobitume Congress, Barcelona, Spain*, 2000.
13. SHRP-A-404 Report, "Fatigue Response of Asphalt-Aggregate Mixes," *Strategic Highway Research Program, National Research Council*, 1994.
14. P. C. Hopman, P. A. J. C. Kunst, and A. C. Pronk, "A Renewed Interpretation Method for Fatigue Measurements, Verification of Miner's Rule", *4<sup>th</sup> Eurobitume Symposium in Madrid, Volume 1*, pp. 557-561, October 1989.

15. Y. R. Kim, H. J. Lee, and D. N. Little, "Fatigue Characterization of Asphalt Concrete Using Viscoelasticity and Continuum Damage Theory", *Journal of the Association of Asphalt Paving Technologists*, Vol. 66, pp. 520-569, 1997.
16. K. A. Ghuzlan and S. H. Carpenter, "Energy-derived, Damage-based Failure Criterion for Fatigue Testing", *Transportation Research Record: Journal of the Transportation Research Board*, No. 1723, pp. 141-149, 2000.
17. P. S. Pell and I. F. Taylor, "Asphaltic Road Materials in Fatigue", *Journal of the Association of Asphalt Paving Technologists*, Vol. 38, pp. 371-422, 1969.
18. J. A. Epps and C. L. Monismith, "Influence of Mixture Variables on the Flexural Fatigue Properties of Asphalt Concrete", *Journal of the Association of Asphalt Paving Technologists*, Vol. 38, pp. 423-464, 1969.
19. K. D. Raithby and A. B. Sterling, "The Effect of Rest Periods on the Fatigue Performance of a Hot-Rolled Asphalt under Repeated Loading", *Journal of the Association of Asphalt Paving Technologists*, Vol. 39, pp. 134-152, 1970.
20. K. Majidzadeh, E. M. Kaufmann, and C. L. Saraf, "Analysis of Fatigue of Paving Mixtures from the Fracture Mechanics Viewpoint", *Fatigue of Compacted Bituminous Aggregate Mixtures, ASTM STP 508*, pp. 67-83, 1972.
21. K. D. Raithby and A. B. Sterling, "Laboratory Fatigue Tests on Rolled Asphalt and Their Relation to Traffic Loading", *Roads and Road Construction*, No. 596-597, pp. 219-223, 1972.
22. K. D. Raithby and A. B. Sterling, "Some Effects of Loading History on the Performance of Rolled Asphalt", *Transport and Road Research Laboratory, Report TRRL-LR496*, Crowthorne, England, 1972.
23. K. Majidzadeh and D. V. Ramsamooj, "Mechanistic Approach to the Solution of Cracking in Pavements", *Highway Research Board, Special Report 140*, pp. 143-157, 1973.
24. C. L. Monismith and Y. M. Salaam, "Distress Characteristics of Asphalt Concrete Mixes," *Journal of the*

- Association of Asphalt Paving Technologists*, Vol. 42, pp. 321-350, 1973.
25. P. S. Pell, "Characterization of Fatigue Behavior", *Highway Research Board, Special Report 140, Proceedings of a Symposium on Structural Design of Asphalt Concrete Pavements to Prevent Fatigue Cracking*, pp. 49-64, 1973.
  26. L. H. Irwin and B. M. Gallaway, "Influence of Laboratory Test Method on Fatigue Results for Asphaltic Concrete", *Fatigue and Dynamic Testing of Bituminous Mixtures, ASTM STP 561*, 1974.
  27. B. W. Porter and T. W. Kennedy, "Comparison of Fatigue Test Methods for Asphalt Materials", *Research Report 183-4, Project 3-9-72-183*, Center for Highway Research, University of Texas at Austin, April 1975.
  28. G. W. Maupin and J. R. Freeman, "Simple Procedure for Fatigue Characterization of Bituminous Concrete", *Report No. FHWA-RD-76-102*, Virginia Highway and Transportation Research Council, University Station, Virginia, 1976.
  29. D. G. Phadnavis and C. G. Swaminathan, "The Response of a Bituminous Mixture at Failure to Different Loading Conditions", *Proceedings of the Australian Road Research*, Vol. 7, No. 2, pp. 23-31, June 1977.
  30. F. P. Bonnaure, A. H. J. J. Huibers, and A. Boonders "A Laboratory Investigation of the Influence of Rest Periods on the Fatigue Characteristics of Bituminous Mixes", *Journal of the Association of Asphalt Paving Technologists*, Vol. 51, pp. 104-126, 1982.
  31. A. A. A. Molenaar, "Fatigue and Reflective Cracking due to Traffic Loads", *Journal of the Association of Asphalt Paving Technologists*, Vol. 53, pp. 440-473, 1984.
  32. S. C. S. R. Tangella, J. Craus, J. A. Deacon, and C. L. Monismith, "Summary Report on Fatigue Response of Asphalt Mixtures", *SHRP-A-369 Report*, Strategic Highway Research Program, National Research Council, Washington, D.C., 1990.
  33. D. V. Ramsamooj, "Fatigue Cracking of Asphalt Concrete Pavements", *Journal of Testing and Evaluation*, Vol. 19, No. 3, pp. 231-239, May 1991.

34. C. De La Roche and N. Sanson, "Caractérisation expérimentale de la dissipation thermique dans un enrobé bitumineux sollicité en fatigue", *Document de Recherche LCPC, Sujet No. 2.01.10.4*, p. 136, 1994.
35. A. A. Tayebali, J. A. Deacon, J. S. Coplantz, J. T. Harvey, and C. L. Monismith, "Mix and Mode-of-loading Effects on the Fatigue Response of Asphalt-Aggregate Mixes", *Journal of the Association of Asphalt Paving Technologists*, Vol. 63, pp. 118-151, 1994.
36. A. A. Tayebali, J. A. Deacon, J. S. Coplantz, F. N. Finn, J. T. Harvey, and C. L. Monismith, "Fatigue Response of Asphalt-Aggregate Mixes", *Report SHRP-A-404, Strategic Highway Research Program, National Research Council, Washington D. C.*, 1994.
37. A. A. Tayebali, J. A. Deacon, and C. L. Monismith, "Development and Evaluation of Surrogate Fatigue Models for SHRP A-003A Abridged Mix Design Procedure", *Journal of the Association of Asphalt Paving Technologists*, Vol. 64, pp. 340-366, 1995.
38. H. DiBenedetto, A. Soltani, and P. Chaverot, "Fatigue Damage of Bituminous Mixtures: A Pertinent Approach", *Journal of the Association of Asphalt Paving Technologists*, Vol. 65, pp. 142-158, 1996.
39. C. De La Roche and P. Marsac, "Caractérisation expérimentale de la dissipation thermique dans un enrobé bitumineux sollicité en fatigue", *First International Eurobitume and Euraspalt Congress-Strasbourg*, May 1996.
40. D. N. Little, R. L. Lytton, and Y. R. Kim "Propagation and Healing of Microcracks in Asphalt Concrete and Their Contributions to Fatigue", *Asphalt Science and Technology*, A. M. Usmani, ed., 1997.
41. G. M. Rowe and S. F. Brown, "Validation of the Fatigue Performance of Asphalt Mixtures with Small Scale Wheel Tracking Experiments", *Journal of the Association of Asphalt Paving Technologists*, Vol. 66, pp. 31-73, 1997.
42. J. M. Read and A. C. Collop, "Practical Fatigue Characterization of Bituminous Paving Mixtures", *Journal of the Association of Asphalt Paving Technologists*, Vol. 66, pp. 74-108, 1997.

43. R. Reese, "Properties of Aged Asphalt Binder Related to Asphalt Concrete Fatigue Life", *Journal of the Association of Asphalt Paving Technologists*, Vol. 66, pp. 604-632, 1997.
44. J. A. Deacon, J. T. Harvey, A. A. Tayebali, and C. L. Monismith, "Influence of Binder Loss Modulus on the Fatigue Performance of Asphalt Concrete Pavements", *Journal of the Association of Asphalt Paving Technologists*, Vol. 66, pp. 633-685, 1997.
45. M. L. Hines, C. De La Roche, and P. Chaverot, "Evaluation of Fatigue Behavior of Hot Mix Asphalt with the LCPC Nantes Test Track and SHRP Testing Tools", *Journal of the Association of Asphalt Paving Technologists*, Vol. 67, pp. 717-737, 1998.
46. C. De La Roche, J.M. Piau, and P. Dangla, "Thermal Effects Induced by Viscoelastic Dissipation during Fatigue Tests on Bituminous Mixtures", *6<sup>th</sup> International Symposium on Creep and Coupled Processes, Bialowieza, Poland*, 23-25 September 1998.
47. P. Baburamani, "Asphalt Fatigue Life Prediction Models – A Literature Review", *Research Report ARR 344, Australia*, 1999.
48. D. V. Ramsamooj, "Prediction of Fatigue Performance of Asphalt Concrete Mixes", *Journal of Testing and Evaluation*, Vol. 27, No. 5, pp. 343-348, September 1999.
49. J. A. Sherwood, X. Qi, P. Romero, and K. D. Stuart, "Full-scale Fatigue Testing from FHWA Superpave Validation Study", *Paper presented at the International Conference of Accelerated Pavement Testing, Reno, NV*, October 1999.
50. T. Zhang and L. Raad, "Numerical Methodology in Fatigue Analysis: Basic Formulation", *Journal of Transportation Engineering*, Vol. 125, No. 6, pp. 552-559, Nov/Dec 1999.
51. B. J. Smith and S. A. M. Hesp, "Crack Pinning in Asphalt Mastic and Concrete: Effect of Rest Periods and Polymer Modifiers on the Fatigue Life", *Proceedings of 2<sup>nd</sup> Eurasphalt & Eurobitume Congress, Barcelona, Spain*, Book II, 539-546, 2000.
52. R. M. Rodrigues, "A Model for Fatigue Cracking Prediction of Asphalt Pavements Based on Mixture

- Bonding Energy”, *International Journal of Pavement Engineering*, Vol. 1 (2), pp. 133-149, 2000.
53. P. Romero, K. D. Stuart, and W. S. Mogawer, “Fatigue Response of Asphalt Mixtures Tested by the Federal Highway Administration’s Accelerated Loading Facility”, *Journal of the Association of Asphalt Paving Technologists*, Vol. 69, pp. 212-235, 2000.
  54. A. Sibal, A. Das, and B. B. Pandey, “Flexural Fatigue Characteristics of Asphalt Concrete with Crumb Rubber”, *International Journal of Pavement Engineering*, Vol. 1 (2), pp. 119-132, 2000.
  55. T. Zhang and L. Raad, “Numerical Methodology in Fatigue Analysis: Applications”, *Journal of Transportation Engineering*, Vol. 127, No. 1, pp. 59-66, Jan/Feb 2001.
  56. K. D. Stuart, and W. S. Mogawer, “Validation of the Superpave Asphalt Binder Fatigue Cracking Parameter Using the FHWA’s Accelerated Loading Facility,” *Journal of the Association of Asphalt Paving Technologists*, Vol. 71, pp. 116-146, 2002.
  57. K. A. Ghuzlan and S. H. Carpenter, “Traditional Fatigue Analysis of Asphalt Concrete Mixtures,” Presented at the Transportation Research Board Annual Meeting, Washington D. C., January 2003.
  58. S. H. Carpenter, K. A. Ghuzlan, and S. Shen, “A Fatigue Endurance Limit for Highway and Airport Pavements,” Presented at the Transportation Research Board Annual Meeting, Washington D. C., January 2003.
  59. AASHTO PP2-00, “ Standard Practice for Mixture Conditioning of Hot-Mix Asphalt (HMA)”, *AASHTO Provisional Standards*, April 2000.